

Quantum confinement observed in Ge nanodots on an oxidized Si surface

Alexander Konchenko and Yasuo Nakayama

CREST Japan Science and Technology Agency, Japan, *c/o* Department of Physics, School of Science, The University of Tokyo, 7-3-1 Hongo, Bunkyo-ku, Tokyo 113-0033, Japan

Iwao Matsuda* and Shuji Hasegawa

Department of Physics, School of Science, The University of Tokyo, 7-3-1 Hongo, Bunkyo-ku, Tokyo 113-0033, Japan

Yoshiaki Nakamura and Masakazu Ichikawa

Quantum-Phase Electronics Center, Department of Applied Physics, Graduate School of Engineering, The University of Tokyo, Bunkyo-ku, Tokyo 113-8656, Japan, and CREST Japan Science and Technology Agency, Japan

(Received 3 August 2005; revised manuscript received 7 December 2005; published 24 March 2006)

Quantum-confinement effect in the valence band of germanium nanodots is clearly measured by means of photoemission spectroscopy. The spherical dots of 3–10 nm in diameter were prepared on a 0.3-nm-thick SiO₂ film on Si(111) substrate. Dot-size dependence of the band edge matched the ones expected from the spherical quantum dot model and calculated from the semiempirical simulation recently reported.

DOI: [10.1103/PhysRevB.73.113311](https://doi.org/10.1103/PhysRevB.73.113311)

PACS number(s): 73.22.-f, 79.60.-i

Nanodots of indirect-gap semiconductors such as Ge are widely studied due to their promising applications, especially in optoelectronics.^{1–4} Recently, Ge nanodots on an oxidized Si surface created by a procedure reported by Ichikawa *et al.*⁵ have attracted a wide interest in the Si-based technology. The main advantages are preparation of uniform-size nanodots with very high density (10¹² cm⁻²) and tunable control of dot size ranging from a few nanometers in diameter. A scanning tunneling microscopy (STM) image of such Ge dots are given in Fig. 1(a). Each nanocluster appears as a domelike structure but recent transmission electron microscopy research⁶ has revealed that it is actually a sphere. The distinction is simply because of STM scanning process with a finite tip radius. It is noted that the Ge dot shape is similar to the one embedded in a SiO₂ matrix.¹ Figure 1(c) illustrates a schematic diagram of band offsets for a system of a Ge quantum dot on an oxidized Si substrate.⁵ The quantum dot states are formed due to quantum confinement effect by two barriers of vacuum potential and an insulating energy gap of 0.3-nm-thick SiO₂ film on a Si substrate. The energies of the valence band maximum (VBM) and conduction band minimum (CBM) should be shifted relative to bands of the bulk germanium due to the quantum confinement effect, leading to an increased energy gap. The VBM and CBM of a quantum dot (QD) correspond to energy levels of ground states (GSs) of a confined hole (*h*) and a confined electron (*e*), respectively, and such energy shifts are indicated in Fig. 1(c). There has been vigorous arguments that such QD states or those of Ge nanocrystals in a SiO₂ matrix are responsible for the photoluminescence.^{1–3} However, to date, no experimental investigation exists which can unambiguously identify quantum confinement effect of Ge nanodots. Moreover, the theoretical approaches to this matter are contradictory.

In the present research, we have performed photoemission spectroscopy measurements on Ge QDs prepared by the method of Ichikawa *et al.*⁵ to study their size-dependent electronic structure. Photoemission spectroscopy has been a very powerful tool to study the valence bands of reduced dimen-

sional structures.⁷ It allows independent research on the valence band edge, which is not possible with optical spectroscopy techniques. Through detailed experiments, we have observed a clear energy shift which is quantitatively compatible to quantum confinement effect in the Ge nanodots. Regarding the present system as a model of Ge nanocrystals in a SiO₂ matrix showing infrared photoluminescence (PL), the

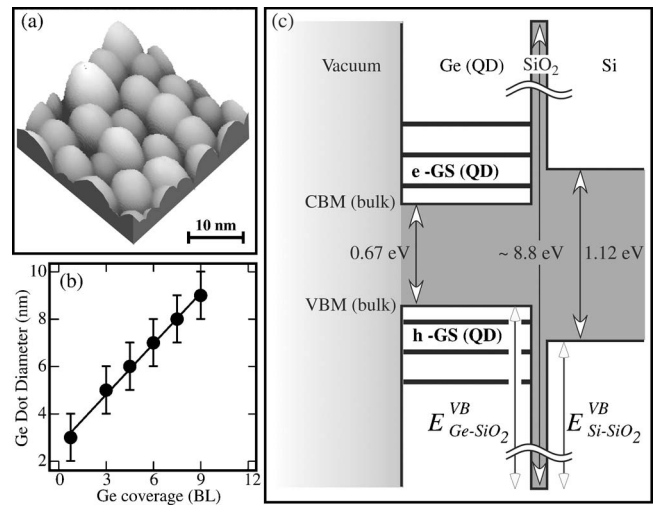


FIG. 1. (a) A STM image of Ge nanodots (QDs) on an oxidized Si(111) surface. Germanium of 3 BL was deposited. (b) Average size of Ge dots with coverage of the Ge deposition. The size is estimated from the STM observation. (c) Schematic band structure of a Ge QD lay between vacuum and an ultrathin SiO₂ film on a Si substrate. Bulk valence band maximum (VBM) and conduction band minimum (CBM) at each material are traced by thin lines. Size of bulk band gaps at room temperature are written for Ge, SiO₂, and Si (Refs. 27, 29, and 30). Ground state (GS) of a confined electron (*e*) or hole (*h*) in a quantum dot (QD) is shown as a thick line. $E_{\text{Si-SiO}_2}^{VB}$ ($E_{\text{Ge-SiO}_2}^{VB}$) indicates the energy difference between VBM of Si and SiO₂ (Ge and SiO₂).

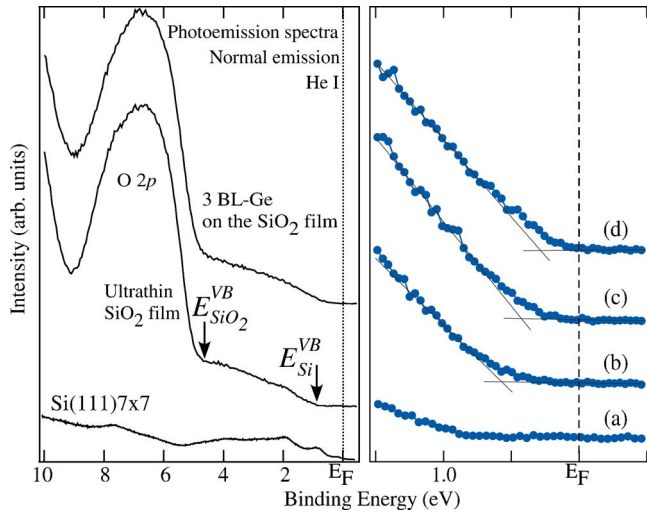


FIG. 2. (Color online) (left) Normal emission photoemission spectra of ultrathin SiO_2 film on $\text{Si}(111)$ before and after 3 BL-Ge deposition. A spectrum of $\text{Si}(111)7 \times 7$ is also shown for a comparison. Spectral features discussed in the text are marked. (right) A collection of normal emission photoemission spectra of an oxidized $\text{Si}(111)$ surface with Ge coverage of (a) 0, (b) 1.5, (c) 4.5, and (d) 7.5 BL. The spectra are normalized by background intensities above E_F , which are proportional to photon flux (Ref. 16).

present result likely supports the PL mechanism of carrier trapping at surface defects.²

Detailed procedures of preparing Ge nanodots on an ultrathin SiO_2 film prepared on a $\text{Si}(111)$ substrate are the same as reported before.⁵ The Si substrate was cut from a mirror-polished n -type $\text{Si}(111)$ wafer ($\sim 10 \Omega \text{ cm}$). First, a clean $\text{Si}(111)7 \times 7$ surface was prepared by a cycle of *in situ* resistive heat treatments in ultrahigh vacuum. Then, the sample temperature was raised from room temperature to 600°C for 10 min after oxygen had been introduced into the chamber at a pressure of 2×10^{-6} Torr. The oxidization procedure results in the formation of 0.3-nm-thick SiO_2 film on $\text{Si}(111)$. Finally, Ge was deposited on the film held at 550°C from an alumina-coated tungsten basket or a Knudsen cell. The Ge coverage or evaporation rate was separately calibrated by reflection high-energy electron diffraction observation of the 5×5 phase prepared by 3 BL-Ge deposition on an annealed $\text{Si}(111)7 \times 7$ surface.^{5,8,9} A relation between the Ge coverage and the Ge dot size was checked by STM, the results of which were consistent with the previous ones.^{5,10} The average dot size has increased with the deposited Ge coverage as shown in Fig. 1(b). STM observation was typically performed with a tip bias of 3 V and a tip current of 0.2 nA. Photoemission spectroscopy measurements were performed with $\text{He I}\alpha$ radiation and a commercial angle-resolved photoelectron spectrometer (VG ADES 400).¹¹ All the photoemission spectra shown in this paper were taken at the normal emission angle. The Fermi level (E_F) was determined from a Ta sample holder plate in good electrical contact with the Si sample. All the measurements were performed at room temperature.

Figure 2 (left) shows an overview of the changes in valence bands by 3 BL-Ge deposition on ultrathin silicon oxide

films. Through a comparison with a spectrum of the clean $\text{Si}(111)7 \times 7$ surface, prominent spectral features for the SiO_2 film are the disappearance of the surface state peaks near E_F and the appearance of a large photoemission peak at binding energy (E_B) of ~ 7 eV. According to previous photoemission reports, the peak is naturally assigned to O $2p$ states of the Si-O-Si bonds in the oxide film.^{12–14} The peak onset (indicated as $E_{\text{SiO}_2}^{\text{VB}}$ in Fig. 2) is located at $E_B = 4.5\text{--}5$ eV and it roughly corresponds to the VBM of the SiO_2 films. Within energy range between $E_{\text{SiO}_2}^{\text{VB}}$ and E_F , there exist photoemission signals which are most likely attributed to bulk states of the $\text{Si}(111)$ substrate. This is supported by the fact that mean free path¹⁵ of the present photoelectron is about 1 nm and it is much longer than the film thickness of ~ 0.3 nm. The signal at $E_B \sim 1$ eV, indicated by $E_{\text{Si}}^{\text{VB}}$ in Fig. 2, seems to be the VBM of the $\text{Si}(111)$ substrate. These results imply that the $E_{\text{Si-SiO}_2}^{\text{VB}}$ (energy difference in VBM between the Si substrate and the SiO_2 film) in Fig. 1 is crudely 3.5–4 eV, which is similar to the ones reported for systems of SiO_2 films on Si surfaces prepared by different procedures.¹⁴

By 3BL-Ge deposition on the SiO_2 film, nanodots with the typical diameter of about 5 nm cover the entire surface as shown in Fig. 1(a). On the other hand, no notable difference can be identified between the two photoemission spectra in Fig. 2 (left). However, focusing on the vicinity of E_F , one can find a systematic change with Ge coverage in Fig. 2 (right). A normalized spectrum of the SiO_2 sample without Ge dots, (a) in Fig. 2 (right), shows no photoemission signal at $E_B < 1$ eV and a small spectral feature of the Si subsurface at $E_B > 1$ eV. On the contrary, large photoemission intensity and obvious spectral edges are detected below binding energy of 0.75 eV for the normalized spectra with Ge nanodots. Furthermore, the VBM approaches to E_F with Ge coverage as given in Figs. 2(b)–2(d). As indicated above with the STM image of Fig. 1(a), the present sample surface consists of two regions (Ge nanodots and bare oxidized surface area) and the measured spectra contains contribution from Ge dots, an oxidized surface, and a Si subsurface. However, the drastic change of spectral features in the normalized spectra indicates that the photoemission intensity near E_F is almost only originated from Ge nanodots. Such spectral appearance of the Ge states is naturally understood from the energy diagram in Fig. 1 that the Ge states (h -GS) exists within the band gap of both the SiO_2 film and the $\text{Si}(111)$ substrate. Furthermore, the systematic shift of the VBM with the Ge dot size obviously indicates the direct observation of the QD states in the present experiment. The spectral feature is broad because photoemission signals from nanodots of different sizes (± 1 nm in diameter) are simultaneously detected at each Ge coverage and the spectrum is given as their summation.^{7,17} The spectral features are similar to the previous photoemission spectroscopy researches of the Si or CdS QDs.^{18–20}

In order to make a quantitative analysis of the experimental results, we have defined, for the sake of convenience, an energy level of the h -GS as an intersection point of two lines extrapolated from spectral tails of the Ge QD valence bands and background signals, Fig. 2 (right). The two lines are

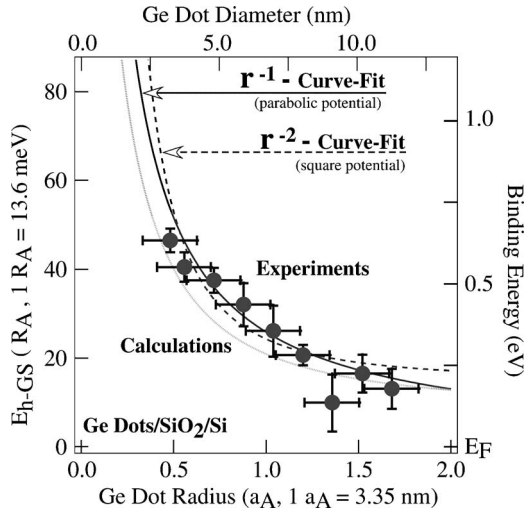


FIG. 3. Energy position change of ground state of holes (h -GS) confined in a Ge quantum dot with average dot size. Experimental data are given by filled circles with error bars. Solid and dashed curves are a least-squares fit by r^{-1} and r^{-2} curves, respectively. The dotted curve is a result of the semiempirical calculation on Ge nanodots reported in Ref. 2. Offset of the calculated curve (Ref. 2) is chosen to match to the r^{-2} -fitted curve at the largest dot size in the figure.

determined by fitting photoemission intensity at $E_B = 0.73$ – 1.2 eV and at nominal binding energy of -0.18 to -0.46 eV (above E_F) in Fig. 2. This analysis provides an accurate amount of binding energy *shift* with QD size but it is difficult to determine the absolute binding energy value.^{18,19,21} The energy positions of the h -GS thus obtained are plotted in Fig. 3 as a function of the average diameter of Ge QDs. It is now clear that the binding energy of the ground state of holes (h -GS) becomes monotonically larger with decreasing the dot size.

There has been many theoretical reports to quantify the electronic state in QDs and the calculations have ranged from using a simple analytical formula to numerical solution of the first principles, depending on a physical/chemical model of a Ge dot.^{2,19,22–25} The most important information is energy levels of h -GS and e -GS since they determine the energy gap for optical properties. Analytical solutions with hard wall square potential and harmonic potential models give that the GS energy is proportional to $r^{-\alpha}$, where r is diameter (radius) of a spherical dot, and the exponent α is 2 and 1, respectively. Theoretical studies of other models have also confirmed that α varies between 1 and 2, depending on calculation methods.^{19,22} In a case of the parabolic potential model of a three-dimensional (3D) spherical dot, energy of the h -GS is expressed by confining potential barrier height, V , and dot radius, r , as^{22,23}

$$E_{h-GS} = E_0 - V + \frac{2\sqrt{V}}{r}, \quad (1)$$

where E_0 is energy reference. The equation is given by the acceptor Rydberg ($R_A = m_h^* \text{Ry} / \epsilon^2$) as a unit of energy, and the acceptor Bohr radius ($a_A = \epsilon a_B / m_h^*$) as a unit of length, where

Ry is the atomic Rydberg, a_B is the atomic Bohr radius, m_h^* is the effective hole valence-band mass, and ϵ is the effective dielectric constant of the semiconductor.^{26,27} In the present paper, we have adopted the conductivity effective mass^{27,28} of holes as m_h^* and bulk dielectric constant of Ge as ϵ .

In Fig. 3, the data points from the photoemission experiments for the defined Ge h -GS are summarized. The data are given in the unit of $R_A (= 13.6 \text{ meV})$ and $a_A (= 3.35 \text{ nm})$. The h -GS energy level monotonically approaches E_F with the QD size. We have made a least-squares fit of the experimental data with r^{-1} and r^{-2} curves. Since the experimental energy positions in Fig. 3 are determined from the spectral edge at smaller binding energy, dot-size errors of only larger ones in Fig. 1(b) are included in the curve-fit. As shown in Fig. 3, the data points clearly follow the expected r -dependence though we cannot distinguish between r^{-1} and r^{-2} dependence. Furthermore, from Eq. (1), we have phenomenologically determined a confining potential of a positive charge (a hole) of the QD is about 2 eV from a coefficient of the r^{-1} term (the $E_0 - V$ value is unnecessary to determine in the present procedure). From the energy diagram in Fig. 1, the energy difference, $E_{\text{Ge-SiO}_2}^{VB}$, may correspond to the confining potential and it matches to the experimental value in the order of magnitude. On the other hand, a semiempirically calculated² curve for a free-standing Ge quantum dot is also shown in Fig. 3 and it consistently matches the experimental results. In order to comprehend the difference between the previous tight binding model² and the present harmonic potential model, we have performed a curve-fit of the calculation curve in Fig. 3 with the function of Eq. (1) in the same dot size range. Then, we have found that $V \sim 1$ eV, which is also similar to the aforementioned value. Despite the lack of a proper definition on the confining energy barrier of a hole in a free standing Ge dot, it may imply that the present V value of ~ 2 eV can be regarded as an empirical parameter to apply the 3D spherical harmonic potential model in the Ge quantum dot system.

Finally, we discuss PL of Ge nanodots from the present research. It has been argued recently that the near-infrared PL from Ge nanocrystals (1–5 nm in diameter) embedded in SiO_2 matrices is originated from the recombination of electron-hole pairs between quantum-confined states³ or involving the trapping on a surface defect.² Takeoka and co-workers have reported a size dependent PL, which seems consistent with the quantum confinement model.³ However, Niquet and co-workers have insisted on the surface defect model since their *ab initio* and semiempirical calculations are not compatible with the PL experiment. To confirm these scenarios, it is inevitable to study electronic states of Ge nanodots directly by experiments. But measurement such as photoemission spectroscopy is significantly difficult for such Ge nanocrystals inside the insulating material.

Focusing on the present system of Ge nanodots on the SiO_2 film, it is fairly reasonable to regard it as a model of the Ge nanocrystals embedded in SiO_2 matrices. Niquet *et al.* have summarized size-dependent band gaps of the Ge dots determined by the previous PL experiments and their semiempirical calculations, which have shown entirely different behaviors from each other.² It is beyond the present photo-

emission measurement to determine the band gap of the Ge dots and to compare it with them. Assuming the symmetric valence and conduction band changes with dot size, as reported by Bostedt *et al.*,²¹ we found that the present photoemission results match the behavior of the previous calculation in the reference.² Furthermore, as shown in Fig. 3, the photoemission data of the *h*-GS energy level is also almost identical to the calculation one.² Therefore the present result likely supports the mechanism that defects at surfaces of the Ge nanodots are involved in the reported PL bands.³

In conclusion, quantum confinement effect in the valence band of Ge nanodots are experimentally observed by photo-

emission spectroscopy. The shift of the band edge with dot-size has matched to those anticipated by the simple quantum dot theory. The present results will play an important role in understanding the nature of photoluminescence phenomena of Ge dots on a SiO₂ film or in a matrix and, furthermore, in comprehending electronic states of the Ge-dot/Si heterostructures.^{1,2,4,24,25}

This work was supported by Japan Science and Technology Agency and by Japanese Society for the Promotion of Science, and CREST of JST.

*Electronic address: matsuda@surface.phys.s.u-tokyo.ac.jp

¹C. Bostedt, T. van Buuren, J. M. Plitzko, T. Möller, and L. J. Terminello, *J. Phys.: Condens. Matter* **15**, 1017 (2003).

²Y. M. Niquet, G. Allen, C. Delerue, and M. Lannoo, *Appl. Phys. Lett.* **77**, 1182 (2000).

³S. Takeoka, M. Fujii, S. Hayashi, and K. Yamamoto, *Phys. Rev. B* **58**, 7921 (1998).

⁴M. Zacharias and P. M. Fauchet, *Appl. Phys. Lett.* **71**, 380 (1997).

⁵A. A. ShklyaeV and M. Ichikawa, *Surf. Sci.* **514**, 19 (2002).

⁶N. Tanaka and M. Ichikawa (unpublished).

⁷I. Matsuda, H. W. Yeom, T. Tanikawa, K. Tono, T. Nagao, S. Hasegawa, and T. Ohta, *Phys. Rev. B* **63**, 125325 (2001); I. Matsuda, T. Tanikawa, S. Hasegawa, H. W. Yeom, K. Tono, and T. Ohta, *e-J. Surf. Sci. Nanotechnol.* **2**, 169 (2004).

⁸Y. Kajiyama, Y. Tanishiro, and K. Takayanagi, *Surf. Sci.* **222**, 47 (1989).

⁹Y. Nakamura, Y. Nagadomi, K. Sugie, N. Miyata, and M. Ichikawa, *J. Appl. Phys.* **95**, 5014 (2004).

¹⁰A. A. ShklyaeV, M. Shibata, and M. Ichikawa, *Phys. Rev. B* **62**, R1540 (2000).

¹¹I. Matsuda, H. Morikawa, C. Liu, S. Ohuchi, S. Hasegawa, T. Okuda, T. Kinoshita, C. Ottaviani, A. Cricenti, M. D'angelo, P. Soukiassian, and G. Le Lay, *Phys. Rev. B* **68**, 085407 (2003).

¹²K. Sakamoto, S. Doi, Y. Ushimi, K. Ohno, H. W. Yeom, T. Ohta, S. Suto, and W. Uchida, *Phys. Rev. B* **60**, R8465 (1999).

¹³K. Sakamoto, H. M. Zhang, and R. I. G. Uhrberg, *Phys. Rev. B* **70**, 035301 (2004).

¹⁴J. W. Keister, J. E. Rowe, J. J. Kolodziej, H. Niimi, T. E. Madey, and G. Lucovsky, *J. Vac. Sci. Technol. B* **17**, 1831 (1999).

¹⁵A. Zangwill, *Physics at Surfaces* (Cambridge University Press,

New York, 1988).

¹⁶I. Matsuda, H. W. Yeom, K. Tono, and T. Ohta, *Phys. Rev. B* **59**, 15784 (1999).

¹⁷I. Matsuda, H. W. Yeom, K. Tono, and T. Ohta, *Surf. Sci.* **438**, 231 (1999).

¹⁸T. van Buuren, L. N. Dinh, L. L. Chase, W. J. Siekhaus, and L. J. Terminello, *Phys. Rev. Lett.* **80**, 3803 (1998).

¹⁹S. A. Ding, M. Ikeda, M. Fukuda, S. Miyazaki, and M. Hirose, *Appl. Phys. Lett.* **73**, 3881 (1998).

²⁰V. L. Colvin, A. P. Alivisatos, and J. G. Tobin, *Phys. Rev. Lett.* **66**, 2786 (1991).

²¹C. Bostedt, T. van Buuren, T. M. Willey, N. Franco, L. J. Terminello, C. Heske, and T. Möller, *Appl. Phys. Lett.* **84**, 4056 (2004).

²²M. Ciurla, J. Adamowski, B. Szafran, and S. Bednarek, *Physica E (Amsterdam)* **15**, 261 (2002).

²³J. Adamowski, M. Sobkowicz, B. Szafran, and S. Bednarek, *Phys. Rev. B* **62**, 4234 (2000).

²⁴J. Y. Kim and J. H. Seok, *Mater. Sci. Eng., B* **89**, 176 (2002).

²⁵M. M. Rieger and P. Vogl, *Phys. Rev. B* **48**, 14276 (1993).

²⁶C. Kittel, *Introduction to Solid State Physics*, 6th ed. (Wiley, New York, 1986).

²⁷S. M. Sze, *Physics of Semiconductor Devices*, 2nd ed. (Wiley, New York, 1981).

²⁸B. Lax and J. G. Mavroides, *Phys. Rev.* **100**, 1650 (1955).

²⁹N. W. Ashcroft and N. D. Mermin, *Solid State Physics* (Saunders College Publishing-Harcourt Brace College Publishing, Orlando, Florida, 1976).

³⁰S. Miyazaki, H. Nishimura, M. Fukuda, L. Ley, and J. Ristein, *Appl. Surf. Sci.* **113/114**, 585 (1997).